AD-A168 963 PLASMA-ENHANCED DEPOSITION AND PROCESSING OF TRANSITION METALS AND TRANSI.. (U) CALIFORNIA UNIV BERKELEY DEPT OF CHEMICAL ENGINEERING D W HESS 20 MAY 86 ARO-19996.9-MS 1/1

UNCLASSIFIED DAAG29-83-K-0039 F/G 20/12 NL

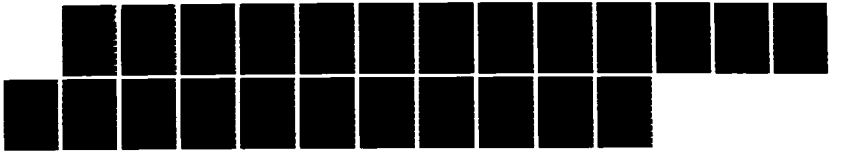

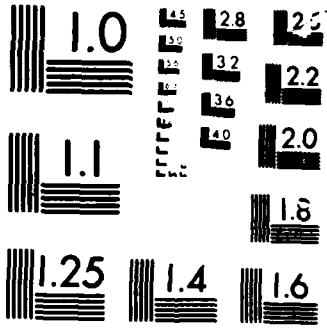
1.0
1.1
1.25
1.4
1.6
1.8
2.0
2.2
2.8
3.2
3.6
4.0

PLASMA-ENHANCED DEPOSITION AND PROCESSING OF TRANSITION METALS AND TRANSITION METAL SILICIDES FOR VLSI

Dennis W. Hess

Contract DAAG29-83-K-0039

1 February 1983 — 31 January 1986

U. S. ARMY RESEARCH OFFICE

ELECTRONICS RESEARCH LABORATORY

College of Engineering
University of California, Berkeley, CA 94720

UNCLASSIFIED

SECURITY CLASSIFICATION OF THIS PAGE (When Data Entered)

AD-A168 963

REPORT DOCUMENTATION PAGE		READ INSTRUCTIONS BEFORE COMPLETING FORM
1. REPORT NUMBER ARO 19996.9-MS	2. GOVT ACCESSION NO. N/A	3. RECIPIENT'S CATALOG NUMBER N/A
4. TITLE (and Subtitle) Plasma-Enhanced Deposition and Processing of Transition Metals and Transition Metal Silicides for VLSI		5. TYPE OF REPORT & PERIOD COVERED Final 1 Feb 1983 to 31 Jan 1986 6. PERFORMING ORG. REPORT NUMBER
7. AUTHOR(s) Dennis W. Hess		8. CONTRACT OR GRANT NUMBER(s) DAAG29-83-K-0039
9. PERFORMING ORGANIZATION NAME AND ADDRESS Department of Chemical Engineering University of California Berkeley, California 94720		10. PROGRAM ELEMENT, PROJECT, TASK AREA & WORK UNIT NUMBERS
11. CONTROLLING OFFICE NAME AND ADDRESS U.S. Army Research Office Post Office Box 12211 Research Triangle Park, NC 27709		12. REPORT DATE May 20, 1986 13. NUMBER OF PAGES 18
14. MONITORING AGENCY NAME & ADDRESS(if different from Controlling Office)		15. SECURITY CLASS. (of this report) Unclassified 15a. DECLASSIFICATION/DOWNGRADING SCHEDULE

16. DISTRIBUTION STATEMENT (of this Report)

Approved for public release; distribution unlimited.

17. DISTRIBUTION STATEMENT (of the abstract entered in Block 20, if different from Report)

NA

18. SUPPLEMENTARY NOTES

The view, opinions, and/or findings contained in this report are those of the author(s) and should not be construed as an official Department of the Army position, policy, or decision, unless so designated by other documentation.

19. KEY WORDS (Continue on reverse side if necessary and identify by block number)

Plasma-enhanced etching
Plasma-enhanced deposition
Transition metal films
Transition metal silicide films

20. ABSTRACT (Continue on reverse side if necessary and identify by block number)

(See reverse side)

DD FORM 1 JAN 73 1473 EDITION OF 1 NOV 65 IS OBSOLETE

UNCLASSIFIED

SECURITY CLASSIFICATION OF THIS PAGE (When Data Entered)

20. *Abstract*

Radiofrequency (rf) discharges have been used to deposit films of tungsten, molybdenum, and titanium silicide. As-deposited tungsten films, from tungsten hexafluoride and hydrogen source gases, were metastable (β-W), with significant (>1 atomic percent) fluorine incorporation. Film resistivities were 40-55 $\mu\Omega$-cm due to the β-W, but dropped to ~8 $\mu\Omega$-cm after a short heat treatment at 700°C which resulted in a phase transition to α-W (bcc form). The high resistivity (>10,000 $\mu\Omega$-cm) associated with molybdenum films deposited from molybdenum hexafluoride and hydrogen appeared to be a result of the formation of molybdenum trifluoride in the deposited material. Titanium silicide films formed from a discharge of titanium tetrachloride, silane, and hydrogen, displayed resistivities of ~150 $\mu\Omega$-cm, due to small amounts of oxygen and chlorine incorporated during deposition. Plasma etching studies of tungsten films with fluorine-containing gases suggest that the etchant species for tungsten in these discharges are fluorine atoms.

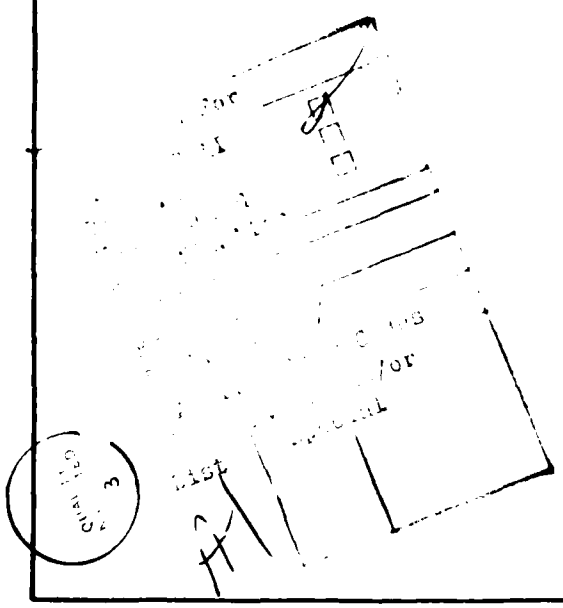

PROBLEM STATEMENT

As silicon device geometries shrink to less than one micron in size, an increasing burden is placed upon the materials used for gates, interconnects, and contacts in MOS circuits. For the past decade, heavily doped polycrystalline silicon and/or aluminum have been the preferred materials for these applications. However, polysilicon is a relatively high resistivity material, thereby reducing speed, and aluminum is a low melting material, thereby limiting processing latitude. As a result, transition metals and transition metal silicides are being studied as possible replacements for current interconnect technology. The following report describes an investigation of the use of rf flow discharges (plasmas) for the deposition of tungsten molybdenum, and titanium silicide films. Chemical, physical, and electrical properties of the films are reported as a function of plasma deposition parameters. In addition, preliminary rf glow discharge etch studies of tungsten films are presented.

INTRODUCTION

The tremendous increase in complexity of integrated circuits (IC's) over the past decade has in large part been made possible by the continual decrease in circuit element or pattern size. As device geometries shrink still further (to 1 μm and less), increasing demands are placed upon the materials used for interconnections and gates in metal-oxide-semiconductor (MOS) circuits. For instance, these materials must possess low resistivity, tolerate high (>600°C) processing temperatures, and be capable of precise and reproducible pattern definition at the 1 μm level.

Since the late 1960's, the material which has been most widely used for interconnect applications is polycrystalline silicon (1). Several reasons exist for its wide utility in this regard. The process technology required for reproducible and controllable deposition of polysilicon is well-established and reasonably well-understood. Also, polysilicon is capable of withstanding high processing temperatures, and can be patterned with existing etchants. Finally, thermal oxidation of polysilicon is easily performed, and the resulting oxide is an insulator with low conductivity, low pinhole density, and excellent adhesion. Therefore, this thermal oxide can be used for masking purposes during polysilicon etching, as well as for dielectric isolation between subsequent films deposited over polysilicon.

However, silicon-gate technology presents several limitations for future (and in some cases present-day) circuits. First, the speed of a circuit is related to the sheet resistance of the interconnect lines. For polysilicon of 0.4 μm thickness and 3 μm width, sheet resistance is fairly high (usually ~100 $\Omega/\square$), and so the propagation delay is high also. Secondly, as devices are scaled to smaller lateral dimensions, the vertical dimensions must also shrink if fine pattern sizes are to be controllably delineated. Thus, sheet resistance increases further, as does the propagation delay. Finally, since the grain size of polysilicon is typically ~0.1 μm under current process conditions, very small lines with straight edges are difficult to achieve.

Two approaches are being pursued to eliminate the disadvantages incurred in polysilicon technology: transition metals and transition metal silicides. Refractory metals such as molybdenum, tantalum, and tungsten have been routinely deposited by sputtering (3-5), electron-beam evaporation (5, 6), and chemical vapor deposition (7-12). These films have proved useful for MOS devices because of their low sheet resistance and small grain size. In particular, these metals are of interest for contact layers, and the potential for selective deposition is most attractive from a processing standpoint (13). However, these metals have higher work functions than does doped polysilicon, and so threshold voltages are naturally higher for unimplanted NMOS circuits. Further, a doped oxide glass must be used for dielectric isolation of the refractory metals from subsequently deposited conducting films, since thermal oxides of these refractory metals are poor dielectric and passivation layers. Finally, these metals are not, in general, resistant to chemical reagents or oxidizing atmospheres used for device processing.

Transition metal silicides have recently generated interest for interconnection technology, either as a single layer film or as a polycide structure (14-19). The silicides have been deposited primarily by electron beam evaporation and sputtering, although CVD has also been used. Resistivities of such silicides as $TaSi_2$, $TiSi_2$, $MoSi_2$, and WSi_2 are in the range of 25-100 $\mu\Omega$-cm (15), which is a factor of 5-10 lower than that of heavily-doped polysilicon.

In addition to the low resistivities and small grain sizes displayed by certain metal silicides, these materials also offer some advantages over refractory metals. For instance, oxidation of the sili-

cides results in a uniform, adherent film of silicon dioxide (15, 20-23). Further, the silicides are relatively inert to normal chemical reagents used for IC processing.

Most of the published work on metal silicides has been carried out on the disilidies. However, unique properties (resistivity, stress, oxidation rate, work function, etc.) may be imparted to these materials if the metal to silicon ratio is varied, and selected impurities are incorporated into the films. Indeed, Murarka (15, 20) has shown that the stress of titanium silicide and tantalum silicide films varies with composition for co-sputtered layers.

Plasma-enhanced chemical vapor deposition (PECVD) has been shown to be an extremely useful technique for the deposition of inorganic dielectric and semiconductor films for integrated circuit and solar cell applications. However, little work has been published on PECVD of metal and metal silicide films. Our studies on PECVD tungsten (23-27) have indicated that relatively low resistivity, unique (metastable) metal films can be formed by PECVD. Further, a few publications on PECVD of metal silicide layers have shown the feasibility of such materials (28-33). Clearly, PECVD offers the potential to systematically vary the important chemical, physical, and electrical properties of transition metal silicide films, and should afford excellent step coverage for these layers.

This report summarizes our work to date on the processing of transition metal and transition metal silicide films by plasma techniques. Although much of this effort has been devoted to PECVD, some preliminary studies on metal etching have also been performed.

RESEARCH RESULTS

Tungsten

Film Deposition

A radial flow parallel plate plasma reactor (described previously (23)) was used for the deposition of tungsten and molybdenum films. Unless otherwise indicated, the following "standard" deposition conditions were used for the tungsten studies described below: T = 350°C, P = 200 mTorr, power = 0.06 W/cm^2, H_2/WF_6 = 3, and f = 4.5 MHz.

Over the temperature range of 200°-400°C, the tungsten deposition rate follows an Arrhenius expression

$$\text{D. R. (nm/ min)} = 101 \exp(-0.16\ \text{eV}/\ kT)$$

The effective activation energy for the PECVD process (0.16 eV/atom) is distinctly different from the E_a for atmospheric pressure CVD tungsten (0.69 eV/atom) (34) and from that for LPCVD tungsten (0.71 eV/atom) (13). These results indicate that the rate-limiting step in CVD is different from that in PECVD. Such observations are quite reasonable, since in atmospheric CVD and in LPCVD, the rate-limiting step appears to be hydrogen dissociation on the substrate surface (13, 34). However, in a glow discharge, hydrogen atoms are already present for reaction with WF_x species.

The specific subfluorides generated via electron impact collision depend on the electron energy. Mass spectrometer studies have demonstrated that with 20 eV electrons, the primary fragment of WF_6 is WF_5^+, with the concentration of WF_4^+ lower by a factor of 4. When 50 eV electrons are used, subfluorides down to WF^+ are observed, although the primary fragment is still WF_5^+. Since the average electron energy in rf glow discharges used for deposition or etching is several electron volts and since few electrons in such plasmas possess energies in excess of 30 eV, the principal fragment in WF_6 glow discharges is apparently WF_5. Indeed, WF_5 appears to be the important intermediate in CVD of tungsten from WF_6 (35).

Dissociation of WF_6 to generate fluorine atoms results in a limitation in the use of the glow discharge technique for tungsten deposition in VLSI. It is well-known that fluorine atoms etch both Si and SiO_2. The etch rates can be expressed by (36, 37):

$$R_F(Si) = 2.91 \times 10^{-13} T^{1/2}\, n_F \exp(-0.108\ \text{eV}/\ kT)$$

$$R_F = (SiO_2) = 8.97 \times 10^{-14} T^{1/2}\, n_F \exp(-0.163\ \text{eV}/\ kT)$$

where R is the fluorine atom etch rate in nm/min, T the temperature in °K, n_F the fluorine atom density in cm^{-3}, and k is Boltzmann's constant. At room temperature (300°K), the etch rates for $n_F = 10^{15} cm^{-3}$ are therefore $R_F(Si)$ = 77 nm/min and $R_F(SiO_2) \cong 3$ nm/min. However, at a typical tungsten deposition temperature of 350°C, R_F (Si), = 968 nm/min and $R_F(SiO_2)$ = 106 nm/min. In

addition, the etch rates are accelerated in the plasma atmosphere. This means that substantial etching of exposed Si or SiO_2 may occur during the initial stages of PECVD. Indeed, over 70 nm of SiO_2 have been removed during the typical deposition cycle of PECVD tungsten.

Under the proper substrate surface preparation and CVD conditions, tungsten can be deposited selectively on Si but not on neighboring oxide regions (38). Preliminary studies have not identified similar conditions in the PECVD process. In fact, selective deposition may not be possible in parallel plate PECVD reactors due to ion bombardment, which can create surface damage and thus adsorption sites on SiO_2.

In order to determine the conformality of PECVD tungsten films over silicon steps. RIE was used to form 1.8 μm and 0.2 μm steps in single crystal and polycrystalline silicon films, respectively. Tungsten films 300 nm thick were then deposited by PECVD over the steps, the samples cleaved, and the cross-sections examined by SEM (24). In both cases, complete conformality by the thin films was obtained

Structure

Scanning electron microscope (SEM) studies of cross sections PECVD tungsten films indicate that the films are columnar, consistent with tungsten films deposited by other techniques (39). SEM investigations show that the grain size of 200 nm-thick PECVD films deposited between 200° and 400°C, is in the range of 20-40 nm. Subsequent heat treatments for 30 min. in N_2/H_2 atmospheres at a temperature of 900°C results in grain growth, with the average grain size in the range 60–70 nm.

As indicated in our previous report, and in Ref. (26), forming gas (10% H_2/90% N_2) heat treatments of as-deposited tungsten films above 500°C significantly reduce the resistivity (from 50 to 13 $\mu\Omega$-cm at 650°C). The activation energy for this resistivity change is ~0.75 eV/molec, which is similar to the reported (40) activation energy for the surface diffusion of tungsten on tungsten (~0.8 eV/atom). X-ray diffraction studies (Fig. 1) have identified the as-deposited PECVD material as β–W, a metastable phase with an A15 or A_3B crystal structure (27). To our knowledge, this is the first report of a metastable elemental phase formed by PECVD. The metastable material is

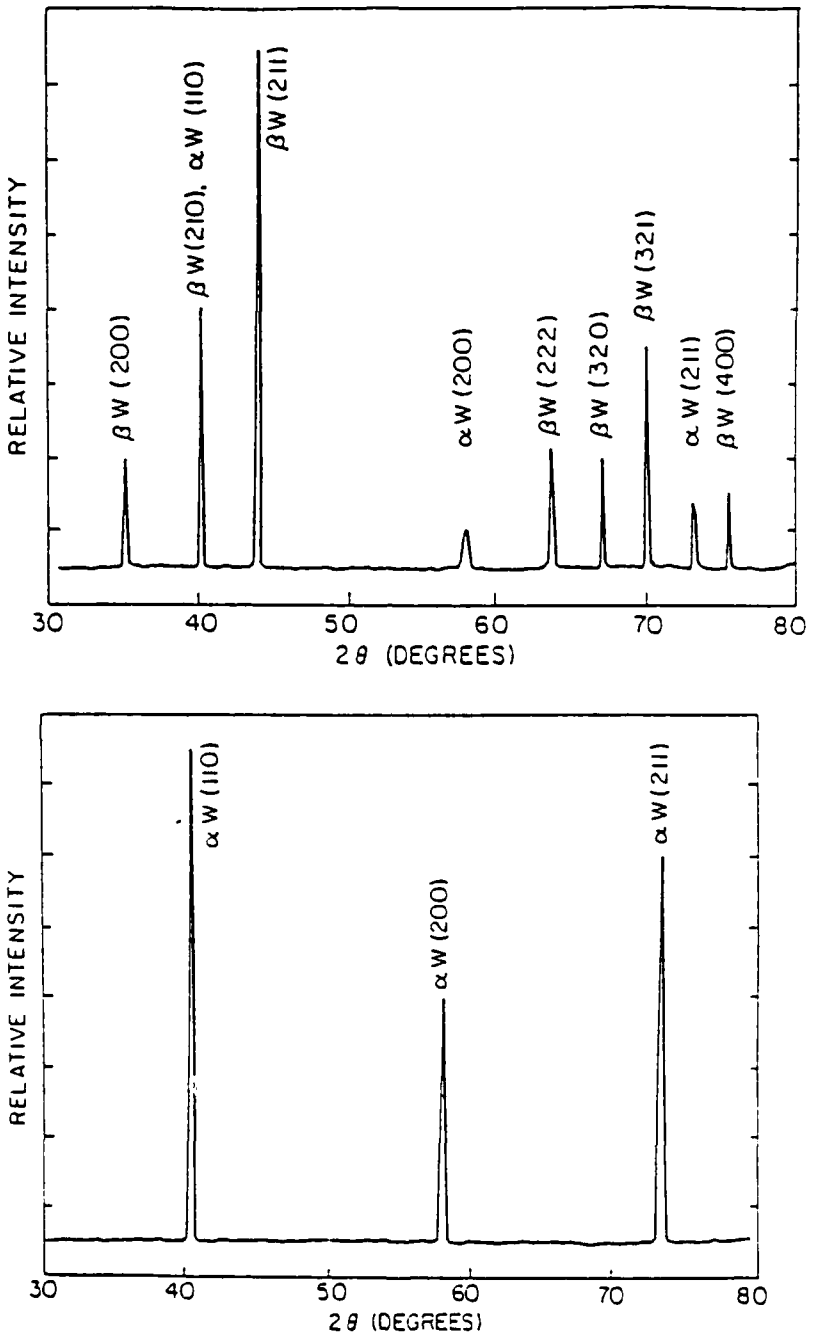

Figure 1. X-ray diffraction patterns of PECVD tungsten film. Top - as-deposited at 350°C; Bottom - after 30 min. in H_2/N_2 at 750°C.

converted into the stable, lower resistivity bcc form upon heat treatments above 600°C, thus accounting for the drop in resistivity described above.

Preliminary XPS (ESCA) studies indicate that as-deposited PECVD tungsten films contain between 1.5 and 1.2 atom percent fluorine, and that the concentration drops to 0.5% upon forming gas heat treatments at 650°C or above, as shown in Fig. 2. Thus, it appears that the presence of fluorine assists the stabilization of the metastable phase, similar to that observed for oxygen impurities in sputtered β-W (41). Outdiffusion of fluorine occurs during heat treatment, thereby permitting the phase transformation. In contrast, tungsten deposition in the reactor without ignition of the discharge results in the formation of only α-W (the stable bcc form) indicating the importance of the plasma atmosphere in nucleation of the metastable phase.

Plasma Etching

PECVD tungsten films were etched in glow discharges containing CF_4 or SF_6 (42). The reactor utilized was the one in which the tungsten depositions were performed (23). Since no cooling capabilities were available in this reactor, the minimum electrode temperature used for the etching studies was 60°C. This temperature allowed etch times greater than 15 min. to be used without a detectable increase in electrode temperature. In order to separately evaluate the effect of various plasma parameters on tungsten etch rates and fluorine atom densities, a set of standard etch conditions was established: 0.2 W/cm^2 at 4.5 MHz, 200 mTorr pressure, 60°C electrode temperature, and a total flow rate of 75 sccm. Optical emission studies were performed with a plasma-Therm PSS-2 system. Relative fluorine atom densities were determined by using argon (2% of the feed gas) as a tracer or "actinometer," and recording emission intensities of Ar (750.4 nm) and F (703.7 nm) as a function of plasma parameters (43). *No change in F atom emission intensity was observed for Ar addition up to 4%.*

The etch depth of tungsten films in SF_6/O_2 plasmas increases linearly with etch time. Further, when this linear relationship is extrapolated, the line passes through the origin, indicating that no initiation period or lag time exists at the start of tungsten etching. This result is consisted with the fact that the etch product (WF_6) is thermodynamically more stable than the oxides (WO_2, WO_3,

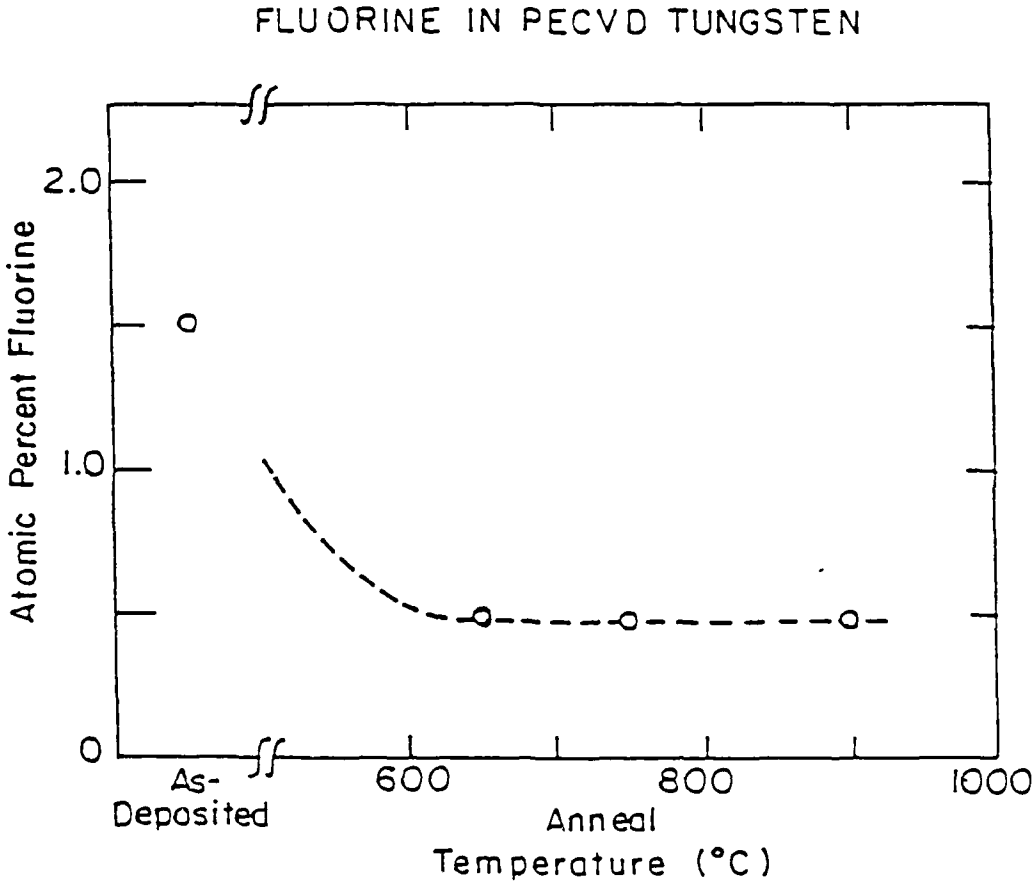

Figure 2. Fluorine content in PECVD tungsten as determined by XPS. Anneal time in H_2/N_2 was 30 min.

W_2O_5) and that tungsten oxyfluorides are volatile.

Arrhenius plots of the etch rate of tungsten in 90% SF_6/10% O_2 and in 90% CF_4/10% O_2 plasmas are shown in Fig. 3. The apparent activation energy for both etchant gases is 0.2 eV/mol. These results suggest that the active etchant species (F) and the reaction mechanism may be the same for both etch gases. Optical emission studies indicate that the higher etch rates observed with SF_6 over CF_4 plasmas are due to higher F atom concentrations in SF_6 discharges.

The effect of oxygen additions to CF_4 on the relative fluorine atom density as determined by actinometry, and on the tungsten etch rate is shown in Fig. 4. Although both fluorine atom density and etch rate go through a maximum, the peak etch rate does not coincide with the maximum fluorine atom density. Such trends are identical to those observed in CF_4/O_2 plasma etching of silicon (44, 45). These results also substantiate the claim that F atoms are the primary etchant for tungsten in CF_4/O_2 discharges. As in the case of Si etching (44), oxygen additions to CF_4 enhance the production of F atoms and reduce C-containing residues, thereby increasing the tungsten etch rate. Further, since F and O atoms compete for surface adsorption sites, a non-coincidence of the tungsten etch rate and the maximum F atom concentration results, *exactly* analogous to that observed in silicon etching (44).

Similar F atom density results to those observed in CF_4/O_2 discharges are noted for SF_6/O_2 plasmas, as shown in Fig. 5. However, the maximum etch rate occurs with a pure SF_6 discharge, in agreement with results reported for reactive ion etching of tungsten (46). In contrast, the maximum F atom density, which is four times higher than in a pure SF_6 discharge, occurs at 30% oxygen. Clearly, competitive adsorption between O and F atoms cannot explain the maximum etch rate at such low O atom concentrations. Since the primary free radicals generated in SF_6 plasmas are apparently SF_5 and SF_3 (47), these species can diffuse to the tungsten surface, where they may undergo dissociative chemisorption to form F, SF_4 and SF_2. These processes can thereby supply additional F atoms to the etching surface most efficiently. Of course, if this process is operative, an alteration of etch mechanism would occur. Indeed, the apparent activation energy for tungsten etching in a pure SF_6 discharge drops by a factor of 3 (to 0.07 eV/mol) compared to SF_6/O_2.

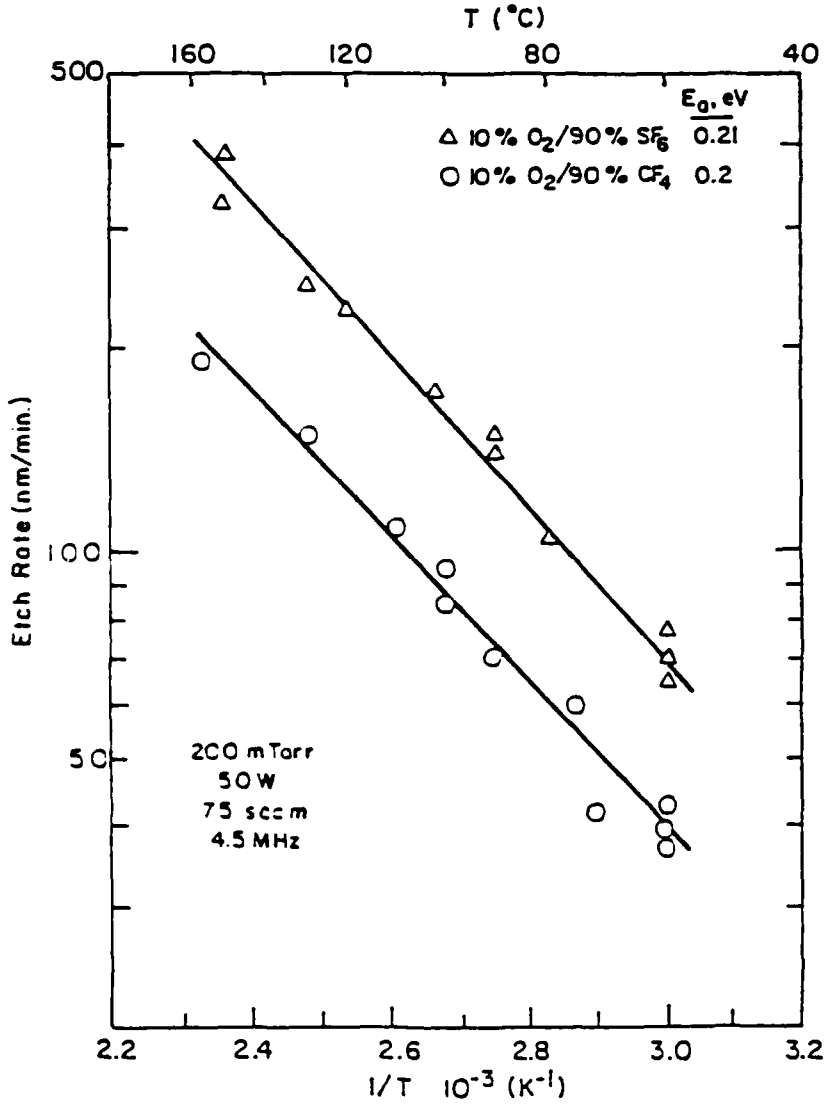

Figure 3. Etch rate of tungsten and relative fluorine atom density as a function of oxygen concentration in CF_4 plasmas.

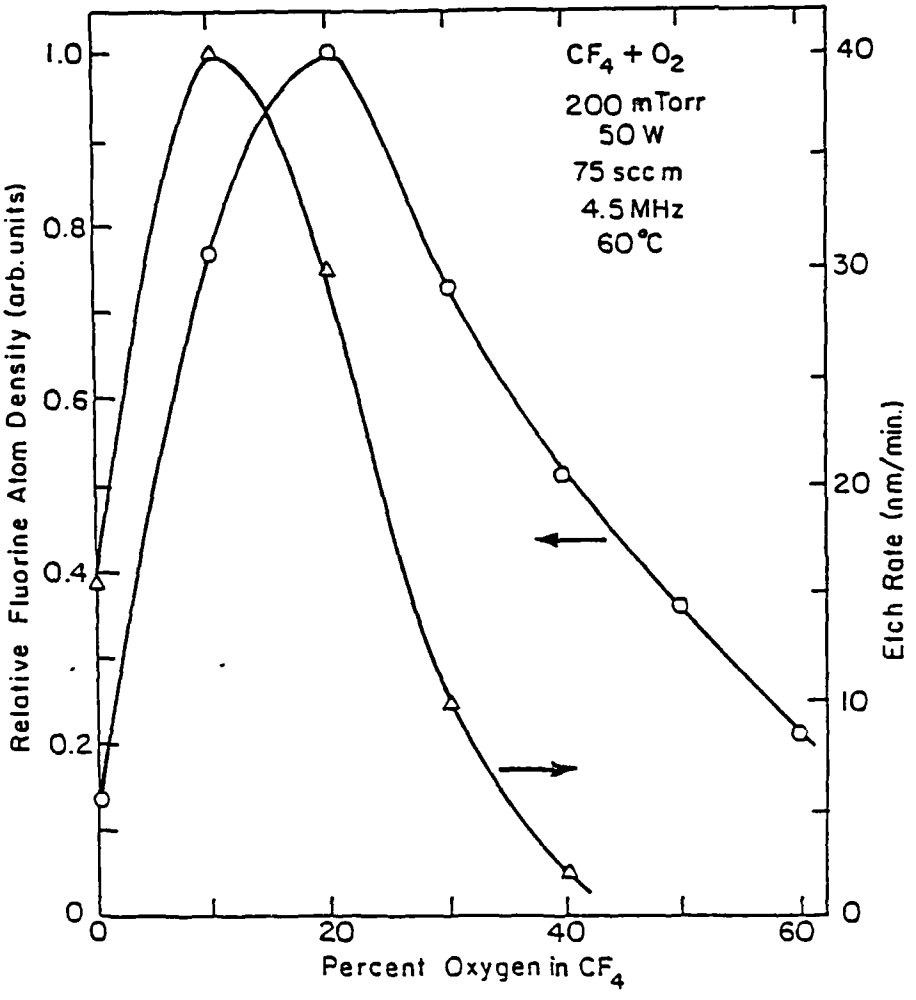

Figure 4. Etch rate of tungsten and relative fluorine atom density as a function of oxygen concentration in CF_4 plasmas.

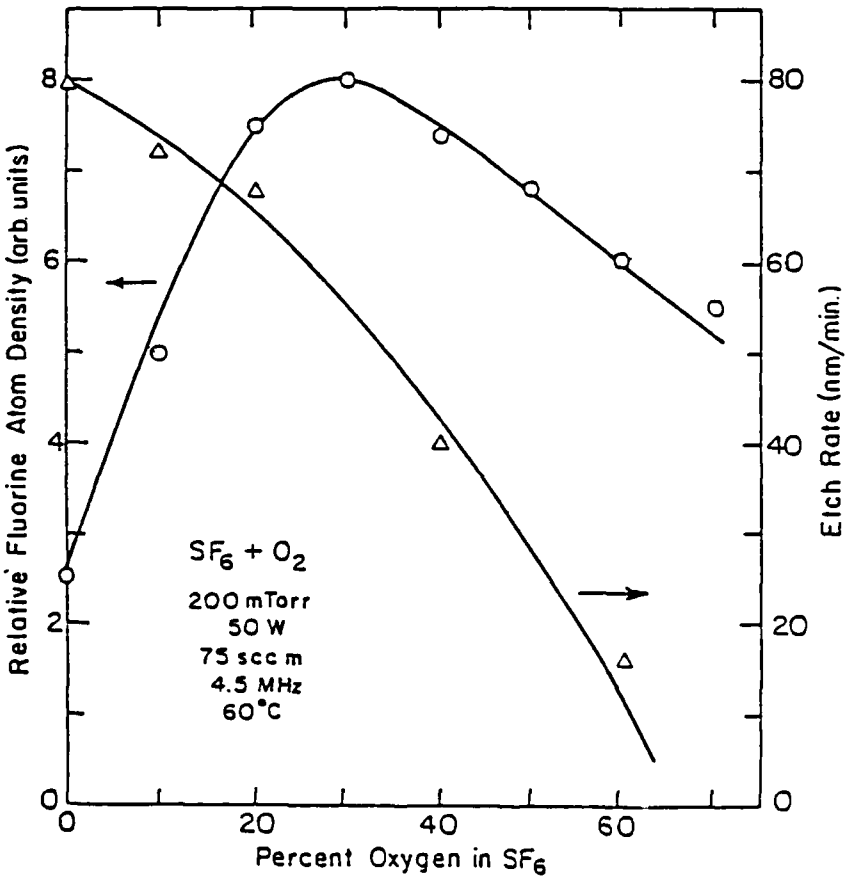

Figure 5. Etch rate and relative fluorine atom density as a function of oxygen concentration in SF_6 plasmas.

Hydrogen addition to CF_4 and SF_6 plasmas result in a scavenging of F atoms, thus decreasing the overall etch rate, and generating residues of carbon or sulfur. However, Auger results suggest that sulfur is easily sputtered from the wafer during etching in SF_6 plasmas at the slightly elevated temperatures used here.

When rf power is increased from 10W to 150W, the F atom density and thus the etch rate in CF_4/O_2 and in SF_6/O_2 discharges increases. Naturally, the etch rates are higher in SF_6 plasmas due to the higher F atom density relative to CF_4 discharges.

The etch rate and the relative F atom density in CF_4/O_2 plasmas both increase linearly with pressure in the range 100-500 mTorr. Unlike CF_4/O_2, the etch rate and relative F atom density in SF_6/O_2 discharges initially increase with pressure and exhibit a maximum at 200 mTorr. Above this pressure, both etch rate and F atom density decrease as the pressure increases. Actinometry results suggest that the electron energy in SF_6 discharges is more sensitive to pressure variation than in CF_4 plasmas. The efficiency of excitation in SF_6 discharges decreases much faster with pressure than in CF_4 discharges, so that fewer F atoms are generated at high (> 200 mTorr) pressures, resulting in a drop in etch rate.

Molybdenum

As described in our last report (July, 1982), we have deposited molybdenum films in an rf discharge of MoF_6 and H_2 (flow ratios greater than 6 H_2/MoF_6) above 200°C electrode temperature (24). The purity of these films is low, with the major contaminant being fluorine; thus the resistivity is high: ~15,000 $\mu\Omega$-cm. Recent XPS studies have indicated that MoF_3 may be incorporated into these films. Indeed, MoF_3 is a stable solid that is not reduced by hydrogen or disproportioned into lower subfluorides below 400°C (48). Further, these conclusions are consistent with reported results of CVD molybdenum films when MoF_6 is used as a reactant (49).

Titanium Silicide

In order to prepare for transition metal silicide deposition by PECVD, we reconfigured the upper (hollow) electrode in our deposition system. The electrode was divided into compartments so

that the two reactants (silane and a transition metal halide) introduced through the electrode did not come into contact until they entered the interelectrode gap and thus the discharge. Such precautions were necessary because of the high reactivity between silane and many transition metal halides.

Parametric studies were conducted on the deposition of $TiSi_x$ from $TiCl_4$, SiH_4 and H_2 (flow ratio of 1:2:70) at a power density of 1.2 W/cm^2. Although an increase in deposition rate from ~3 nm/ min at 250°C to ~60 nm/min at 430°C was observed, the total pressure and rf frequency had the largest effect on deposition rate. For instance, below a total pressure of 0.8 Torr, the deposition rate was less than 1.5 nm/min. As the pressure was increased from 0.9 to 1.7 Torr, the deposition rate increased almost linearly from 2.2 to 9.4 nm/min; similarly, as the rf frequency was increased from 2 to 13.56 MHz, the deposition rate increased essentially linearly from 3.9 to 17.1 nm/min. However, because an increase in pressure and frequency results in lower electron energies and ion bombardment energies, it is expected that a considerable amount of chlorine would be incorporated into the deposited films. Indeed, at pressures above 1.5 Torr, and frequencies above 6 MHz, an increase in as-deposited resistivity was observed. Thus, from our results, it appears that the best compromise for the deposition of $TiSi_x$ films occurred under the following conditions: 1.5 Torr, 1.2 W/cm^2, 430°C, 3 MHz, and flow ratios of 0.6 sccm $TiCl_4$, 1.2 sccm SiH_4, and 40 sccm H_2. Under these conditions, films with as-deposited sheet resistivities between 9 and 11 Ω/□ were formed. This represents a factor of two improvement over previous reportes of PECVD $TiSi_x$ (30).

In the hopes of lowering the sheet resistivity to less than 1 Ω/□ (near bulk resistivity), anneals in N_2/ H_2 at temperatures of 650°C or above were performed. Unfortunately, 2-4 Ω/□ was the lowest sheet resistivity attainable. Auger depth profiles indicated that oxygen was incorporated at the interface between the silicon substrate and the $TiSi_x$ film. Although this did not significantly affect the as-deposited resistivity, anneal cycles above 600°C caused a diffusion of oxygen into the bulk of the film and limited the minimum resistivity to ~3 Ω/□. Such results indicate that it is possible to deposit reasonable quality $TiSi_x$ films via PECVD only if an improved vacuum system is implemented so that oxygen is totally excluded. A possible alternative might be to sandwich the $TiSi_x$ between two layers of polysilicon as reported in a previous study (30).

Auger and RBS studies have demonstrated that the as-deposited Si/Ti ratio is 1.2; this value changes to 2 when anneals above 650°C were performed. In addition, the surface of the $TiSi_x$ film became extremely rough, as evidenced by SEM investigations. We believe that the roughness occurred because of defects or weak spots in the native SiO_2 present on the silicon surface. Such defects permit localized diffusion of silicon into the $TiSi_{1.2}$ film, thereby forming $TiSi_2$ from essentially a "point source." This created large $TiSi_2$ growths and thus a rough surface.

The structure of PECVD $TiSi_x$ films was investigated by X-ray diffraction techniques. As-deposited at 430°C, the films were largely amorphous, although a small peak corresponding to the (311) orientation of $TiSi_2$ was observed. Upon annealing at 800°C in nitrogen, this peak sharpened and grew in intensity. In addition, a peak assigned to the (313) orientation of $TiSi_2$ appeared. A 900°C nitrogen anneal increased the intensity of this peak and another peak, due to the (004) orientation, appeared. No diffraction peaks due to TiSi, Ti_5Si_3, or other silicides were detected. Further, no titanium oxide peaks were observed. Such results are consistent with trends reported for the annealing titanium films evaporated onto silicon substrates.

As-deposted $TiSi_x$ film stress levels were determined by measuring the bowing of a film deposited onto glass cover slips using a metallurgical microscope. The parameters that most affected the stress type and level were the deposition temperature and excitation frequency. Below 400°C, the compressive stress of the film increased as the temperature dropped. Above 400°C, the tensile stress increased with increasing temperature. Such results may be a function of oxygen incorporation at the lower temperature (thus generating compressive stress) and a preponderance of thermal induced stress (yielding tensile stress) as the deposition temperature was increased. As the excitation frequency was decreased from 8 MHz to 1 MHz, the tensile stress level increased. Above ~9 MHz, the stress became compressive. At present, it is unclear why such trends were observed. We expect that the stress level and type were established by ion bombardment flux and energy, but the trends are reversed from those reported for PECVD silicon nitride as a function of frequency.

REFERENCES

1. F. Faggin and T. Klein, Solid State Electron, *13*, 1125 (1970).
2. T. I. Kamins, M. M. Mandurah, and K. C. Saraswat, J. Electrochem. Soc., *125*, 927 (1978).
3. D. M. Brown, W. E. Engeler, M. Garfinkel, and P. V. Gray, Solid State Electron, *11*, 1105 (1968).
4. W. E. Engeler and D. M. Brown, IEEE Trans. Elec. Dev., *ED-19*, 54 (1972).
5. P. L. Shah, *ibid*, *ED-26*, 631 (1979).
6. H. Oikawa, J. Vac. Sci. Technol., *15*, 1117 (1978).
7. T. Sugano, Jap. J. Appl. Phys., *7*, 1028 (1968).
8. D. K. Seto, in *Chemical Vapor Deposition - Third International Conference*, The Electrochemical Society, Inc., 1971, p. 659.
9. J. M. Shaw and J. A. Amick, RCA Review, *31*, 306 (1970).
10. G. Wahl and P. Batzie, *Chemical Vapor Deposition - Fourth International Conference*, The Electrochemical Society, Inc., 1973, p. 425.
11. N. E. Miller and I. Beiglass, Solid State Technol., *23* (12), 79 (1980).
12. M. J. Cooke, Vacuum, *35*, 67 (1985).
13. E. K. Broadbent and C. L. Ramiller, J. Electrochem. Soc., *131*, 1427 (1984).
14. B. L. Crowder and S. Zirinsky, IEEE Trans. Elec. Dev., *ED-26*, 369 (1979).
15. S. P. Murarka, *Silicides for VLSI Applications*, Academic Press, N.Y., 1983.
16. J. Y. Chen and L. B. Roth, Solid State Technol., August 1984, p. 145.
17. M. Y. Tsai, H. H. Chao, L. M. Ephrath, B. L. Crowder, A. Cramer, R. S. Bennett, C. J. Lucchese, and M. R. Wordeman, J. Electrochem. Soc. *128*, 2207 (1981).
18. S. Inoue, N. Toyokura, T. Nakamura, M. Maeda, and M. Takagi, J. Electrochem. Soc., *130*, 1603 (1983).

19. W. I. Lehrer, J. M. Pierce, E. Goo, and S. Justi, "VLSI Science and Technology," ed. by C. J. Dell'Oca and W. M. Bullis, The Electrochem. Soc. Inc., Pennington, 1982, p. 258.

20. S. P. Muraka, J. Vac. Sci. Technol., *17*, 775 (1980).

21. S. Zirinsky, W. Hammer, F. d'Heurle, and J. Baglin, *ibid*, *33*, 76 (1978).

22. F. Mohammadi, K. C. Saraswat, and J. D. Meindl, IEDM Technical Digest, December 3-5, 1979, p. 454.

23. J. K. Chu, C. C. Tang, and D. W. Hess, Appl. Phys. Lett., *41*, 75 (1982).

24. C. C. Tang, J. K. Chu, and D. W. Hess, Solid State Technol., March 1983, p. 125.

25. D. W. Hess, J. Vac. Sci. Technol., *A2*, 244 (1984).

26. D. W. Hess, *VLSI Electronics*, Vol. 8, Academic Press, N.Y., 1984, p. 55.

27. C. C. Tang and D. W. Hess, Appl. Phys. Lett., *45*, 633 (1984).

28. K. Akimoto and K. Watanabe, Appl. Phys. Lett., *39*, 445 (1981).

29. A. Tabuchi, S. Inoue, M. Maeda, and M. Takagi, Jpn. Semicond. Technol. News, February 1983, p. 43.

30. R. S. Rosler and G. M. Engle, J. Vac. Sci. Technol., *B2*, 733 (1984).

31. M. J. Kemper, S. W. Koo, and F. Huizinga, Extended Abstracts, The Electrochem. Soc., Inc., New Orleans, October 7-12, 1984, Abstract No. 377.

32. K. Hieber, M. Stolz, and C. Wieczorek, "Proc. Ninth Int. Conf. on CVD," ed. by Mc.D. Robinson, G. W. Cullen, C. H. J. van den Brekel, J. M. Blocker, Jr., and P. Rai-Choudry, The Electrochem. Soc., Inc., 1984, p. 205.

33. D. W. Hess, Mat. Res. Soc. Symp. Proc., Vol. 38, 1985, p. 315.

34. W. A. Bryant, J. Electrochem. Soc., *125*, 1534 (1978).

35. L. V. McCarty, W. E. Reith, and M. T. Simon, J. Electrochem. Soc., *121*, 1372 (1974).

36. D. L. Flamm, V. M. Donnelly, and J. A. Mucha, J. Appl. Phys., *52*, 3633 (1981).

37. D. L. Flamm, C. J. Mogab, and E. R. Sklaver, J. Appl. Phys., *50*, 6211 (1979).

38. N. Miller and I. Beinglass, Solid State Technol., December 1980, p. 79.

39. P. L. Shah, IEEE Trans. Elec. Dev., *ED-26*, 631 (1979).

40. G. Ehrlich and F. G. Hudda, J. Chem. Phys., *44*, 1039 (1966).

41. P. M. Petroff and W. A. Reed, Thin Solid Films, *21*, 73 (1974).

42. C. C. Tang and D. W. Hess, J. Electrochem. Soc., *131*, 115 (1984).

43. J. W. Coburn and M. Chen, J. Appl. Phys., *51*, 3134 (1980).

44. C. J. Mogab, A. C. Adams, and D. L. Flamm, J. Appl. Phys., *49*, 3796 (1978).

45. R. d'Agostino, F. Cramarossa, S. De Benedicts, and G. Ferraro, J. Appl. Phys., *52*, 1259 (1981).

46. J. W. Randall and J. C. Wolfe, Appl. Phys. Lett., *39*, 742 (1981).

47. J. J. Wagner and W. Brandt, Plasma Chem. Plasma Proc., *1*, 201 (1981).

48. D. E. LaValle, R. M. Steele, M. K. Wilkinson, and H. L. Yakel, Jr., J. Am. Chem. Soc., *82*, 2433 (1960).

49. R. Jaeger and S. Cohen, Proc. 3rd Int. Conf. CVD, F. A. Glask, ed., Amer. Nuc. Soc., New York, 1972, p. 500.

END

DTIC

8-86